Geophys. J. Int. (2004) **157,** 1189–1205 doi: 10.1111/j.1365-246X.2004.02255.x

Coherent-state analysis of the seismic head wave problem: an overcomplete representation and its relationship to rays and beams

C. J. Thomson

Department of Geological Sciences & Geological Engineering, Queen's University, Kingston, ON K7L 3N6*, Canada. E-mail: thomson@geol.queensu.ca*

Accepted 2004 January 16. Received 2004 January 14; in original form 2003 June 18

SUMMARY

The coherent-state transform (CST) is a Gaussian-windowed Fourier transform and compared with the usual plane wave expansion of seismic wavefields it provides an overcomplete basis of partial waves. These overcomplete partial waves have associated rays and the relationship of these rays to those of a physical wave front is explained here by appealing to a familiar analytic example. The exact CST of the standard Fourier plane wave summation for a point-source primary wave can be interpreted as a sum of damped plane waves forming a focussed or beam-like wavefield. This primary wave CST can also be approximated as a bundle of complex rays in a position-slowness space with higher dimension than that usually considered, a consequence of the overcompleteness. The higher-dimensional ray spreading controls the coherent-state (CS) amplitude. This complex-ray bundle in turn can be approximated as a paraxial Gaussian beam carried by a real ray associated with the physical wave front.

The exact CST of the standard plane wave summation for a point-source reflection shows how the complex-ray and paraxial-beam approximations generalize to interfaces. Around a critical angle the standard plane wave summation has an asymptotic form involving the Weber function and this function also necessarily arises in the complex-ray and paraxial-beam approximations for the reflection CST. The inverse CST giving the point-source wavefield is a sum of coherent states and those contributing rays or paraxial beams that are incident around the critical angle should be given a reflection coefficient involving the Weber function. CS beams that are incident away from the critical angle collect a peripheral branch-point diffraction. In general, both types of critical-ray/branch-point signal should be included if the integrated CS response is to correctly describe the head wave.

An advantage of the CST is that it combines with ray theory for gradually varying media to give a convenient solution to the caustic and pseudocaustic problems. It may be said to unify the Maslov and standard Gaussian-beam methods of seismic modelling, in part by avoiding the ray-centered coordinates conventionally employed in the latter. The general idea of such overlapping partial wave expansions, their flexibility and the smoothing they impart may have other benefits in seismic analysis and processing.

Key words: body waves, coherent states, diffraction, Gaussian beams, ray theory, wavefield decomposition.

1 INTRODUCTION

The classic seismic reflection and critical-angle problem (e.g. Červený & Ravindra 1971; Chapman 1978; Brekhovskikh 1980) is used here to exemplify the coherent-state transform in the context of wave propagation, rays and diffracted signals. The coherent-state transform, or CST, is essentially a Gaussian-windowed Fourier transform (Klauder 1987). Although this is a familiar notion when applied to the analysis of a recorded time-series (time-frequency analysis; see for example Kaiser 1994; Keilis-Borok 1989), its use to decompose evolving solutions to the seismic wave equation warrants discussion. This is partly because the CST provides an overcomplete basis of partial waves (the coherent states), which must satisfy their own differential equation. Furthermore, when a ray interpretation is sought it is found that the coherent-state (CS) rays travel in a position-slowness space of higher dimension than the one usually considered, a consequence of the overcompleteness. The ray coordinates even become complex, as suggested by the Gaussian decay in some directions. Despite these conceptual complications, convenient approximations exist that require only real ray tracing and the extra computational effort is minimal because these

real rays correspond to the standard rays of the physical wave front. The difference lies in how their geometrical spreading information is used.

An advantage of the CST is that it efficiently removes both the caustic and pseudocaustic limitations of ray theory (Červený 2001) and Maslov theory (Maslov & Fedoriuk 1981; Chapman & Drummond 1982) in smoothly varying media, which was the original idea of Klauder (1987). Brief overviews of this approach to ray theory have also been given by Klauder (1988) and Foster & Huang (1991), the latter specifically proposing its use in seismology. One could say that pseudocaustics are avoided by pushing them into complex position/slowness space, where they do not affect the validity of the asymptotic solution for real receivers. One could also say that the CST shows how flexibly we may interpret the intuitive idea that a bundle of rays sampling the medium controls the waveform, rather than just a single ray. Within reasonable limits the results should be insensitive to the precise width of the Gaussian window, because the weighting applied to each ray of the bundle is adjusted accordingly.

Seismic data analysis/processing techniques that use plane wave decomposition and extrapolation of the partial waves conceivably will benefit from the smoothing properties of the CST. In migration methods the effects of spurious noisy records and finite apertures (endpoints) could be mitigated. The Green-function estimation needed for waveform inversion via Born scattering and gradient optimization (e.g. Pratt *et al.* 1998) is another natural application. In such applications it will be helpful to know that the forward and inverse CST are exact and that the propagation stage has the flexibility referred to earlier, especially in three dimensions where alternatives may be unwieldy.

In fact, the Gaussian-beam pre-stack migration method of Hill (2001) displays essentially these attributes already. The Gaussian-beam summation (Červený *et al.* 1982; Červený 2001; Nowack 2003) and Maslov–Fourier methods are somewhat similar and one could say the CS method unifies them. The higher dimensional space needed to describe the CS rays is an important conceptual distinction, but the fact that in practice the real rays of the physical wave front will probably suffice brings the method into close agreement with its two predecessors. In an earlier CS paper (Thomson 2001, Paper I), the emphasis was on the direct ray or asymptotic solution of the elastic wave equation in inhomogeneous and anisotropic media, with particular emphasis on the geometrical-spreading concept in the higher dimensional CS ray space. It is hoped that the present less-general and scalar wave description will be a more helpful introduction to the basic ideas and make Paper I more accessible to new readers.

2 NOTATION AND BASIC DEFINITIONS

Consider two homogeneous half-spaces in contact. Let $(x_1, x_2, x_3) = (x_\alpha, x_3) = (x, z)$ be Cartesian coordinates, with $\alpha = 1, 2$ and x denoting the lateral two-vector x_α. It will be understood below that subscript α is often hidden (e.g. in $px = p_\alpha x_\alpha$) and it is expected that the context will make clear if summation, double integration, etc., are implied. This is consistent with the notation in Paper I, where the explicit use of subscripts was generally avoided in the hope that it would clarify the basic structure of the ray geometrical relationships. The depth variable z will also be left implicit in many places. For simplicity let the inhomogeneous wave equation for a point source at $(x = x_S, z = 0)$ take the form

$$\partial_\alpha^2 u + \partial_z^2 u + \frac{\omega^2}{v^2} u = \delta(x - x_S)\,\delta(z), \tag{2.1}$$

where $\partial_\alpha = (\partial/\partial x_1, \partial/\partial x_2)$ and frequency ω is assumed positive real. Let $z = h > 0$ be the depth of the plane boundary and let the wave speeds be v_1 and v_2 in $z < h$ and $z > h$, respectively. The boundary conditions at $z = h$ are a continuity of u and $\partial_z u$.

The transverse 2-D spatial Fourier transform convention is defined by

$$\hat{u}(p) = \int u(x)\, \exp(-\mathrm{i}\omega p x)\, dx \qquad u(x) = \left(\frac{\omega}{2\pi}\right)^2 \int \hat{u}(p)\, \exp(\mathrm{i}\omega p x)\, dp, \tag{2.2}$$

where it is understood that these are double integrals. We introduce the 2-D Gaussian window at position x',

$$g(x, x') = \exp\left[-\frac{1}{2}\omega\Omega(x - x')^2\right], \tag{2.3}$$

and then the windowed Fourier transform is given by

$$\hat{u}(p, x') = \int u(x)\, g(x, x') \exp(-\mathrm{i}\omega p x)\, dx = \psi(p, x') \exp(-\mathrm{i}\omega p x'). \tag{2.4}$$

The new function ψ on the right-hand side here is the CST, essentially as defined by Klauder (1987, eq. 4.1, less a multiplicative scaling factor involving Ω). Making a simple change (shift) of integration variable gives

$$\psi(p, x') = \int u(y + x') \exp\left(-\frac{1}{2}\omega\Omega y^2\right) \exp(-\mathrm{i}\omega p y) dy. \tag{2.5}$$

Taking the inverse Fourier transform of eq. (2.4) yields

$$u(x)\, g(x, x') = \left(\frac{\omega}{2\pi}\right)^2 \int \psi(p, x') \exp[\mathrm{i}\omega p(x - x')]\, dp. \tag{2.6}$$

Because $g(x', x') = 1$, putting $x = x'$ immediately leads to the simplest form of the inverse CST:

$$u(x) = \left(\frac{\omega}{2\pi}\right)^2 \int \psi(p, x)\, dp. \tag{2.7}$$

This is the form discussed by Klauder (1987) and which we use here. However, there are other alternatives that relate closely to the treatment of windowed Fourier transforms given by Kaiser (1994, chapter 2) and the general theory of continuous wavelets. Considered as a function in the (p, x) plane, ψ intuitively contains an overcomplete specification of the original wavefield $u(x)$. For example, slightly adjusting the position x' of the Gaussian window before Fourier transformation in eq. (2.4) does not greatly alter the information about u contained in the result ψ. This overcompleteness is expressed in the theory of wavelets and frames via inverse transforms involving integrations over both scale (in our case the slowness p) and position (in our case the Gaussian centre x'). These alternative forms are briefly discussed by Thomson (2001) and they will not be further mentioned here.

Lastly we need the derivative rule/relationship

$$\partial_x u(x) = \left(\frac{\omega}{2\pi}\right)^2 \int \partial_x \psi(p, x)\, dp \quad [\text{i.e.} \quad \text{CST}(\partial_x u) = \partial_x \psi], \tag{2.8}$$

which is fairly obvious from either eqs (2.5) or (2.7). Note that it concerns differentiation with respect to the second argument of ψ and that from here on we are implicitly using only the first form (eq. 2.7) of the inverse CST, not the others referred to above.

3 TRANSFORMED WAVE EQUATION AND PRIMARY WAVES

3.1 Exact solution

Applying the CST with respect to x (i.e. x_α) to the wave equation (eq. 2.1) and using the derivative rule (eq. 2.8) yields

$$\partial_\alpha^2 \psi + \partial_z^2 \psi + \frac{\omega^2}{v^2}\psi = g(x_S, x) \exp\left[\mathrm{i}\omega p\,(x - x_S)\right] \delta(z), \tag{3.1}$$

where now it is understood that the spatial derivatives on the left-hand side act on the second argument of $\psi(p, x)$. The solution of this equation is quite distinct from that of the original eq. (2.1), even though the differential operator on the left-hand side looks the same. If the medium were laterally inhomogeneous, so that $v^{-1} = v^{-1}(x)$, then a pseudodifferential operator (PSDO) denoted $v^{-1}(x - (\mathrm{i}\omega)^{-1}\partial_p)$ would be introduced by the CST (Thomson 2001 §4.1) and this would amplify the contrast with the untransformed original equation.

Eq. (3.1) is not significantly simplified compared to the original wave equation, in comparison with the simplification usually found by applying the standard Fourier transform. Insight into the form of the solution to eq. (3.1) may be gained by starting with the standard Fourier slowness-integral representation of the primary wave solution to the original wave (eq. 2.1) in the upper layer. Namely

$$u^{\text{inc}}(x, z) = \left(\frac{\omega}{2\pi}\right)^2 \int \frac{1}{2\mathrm{i}\omega q_1} \exp\left\{\mathrm{i}\omega[\tau^{\text{inc}}(p, z) + p(x - x_S)]\right\} dp, \tag{3.2}$$

where $\tau^{\text{inc}}(p, z) = \int_0^z q_1(p)\, dz$ and $q_1(p) = (v_1^{-2} - p^2)^{\frac{1}{2}}$ is the positive vertical slowness for downgoing incident waves (see, for example, Chapman 1978). This form may be regarded as exact for the wave incident at the boundary $z = h > 0$, although it is not an appropriate representation for direct waves to receivers lying near $z = 0$ (i.e. for horizontal rays emanating from the source).

Applying eqs (2.4) or (2.5) to eq. (3.2), changing the integration order (which is allowed for the damped integral) and performing the spatial integration with respect to x yields

$$\psi^{\text{inc}}(p', x') = \left(\frac{2\pi}{\omega\Omega}\right)\left(\frac{\omega}{2\pi}\right)^2 \int \frac{1}{2\mathrm{i}\omega q_1} \exp\left\{\mathrm{i}\omega\left[\tau^{\text{inc}}(p, z) + p(x' - x_S)\right] - (\omega/2\Omega)(p - p')^2\right\} dp, \tag{3.3}$$

and it is straightforward to verify by substitution that this is a solution to eq. (3.1) in $z > 0$. Further, eq. (3.3) can be combined with a corresponding expression for $z < 0$ to show that the jump in $\partial_z \psi$ at $z = 0$ matches as required with the inhomogeneous term in eq. (3.1). Note that the z dependence is left implicit on the left-hand side in eq. (3.3). Also, x' has been kept as the spatial argument in eq. (3.3), to emphasize that it corresponds to the position of the Gaussian spatial window in the basic definition (eq. 2.4). However, the prime will not generally be used below.

Substitution of eq. (3.3) into the inverse CST (eq. 2.7) returns the known Fourier solution (eq. 3.2) rather easily, because the integration over p' separates. However, because eq. (3.3) is itself an integral or sum over partial waves, it clouds the interpretion of what is meant by a coherent state. The Gaussian-windowed oscillatory integrand in eq. (2.4) is an x -space localized wave and we could refer to it as an elemental wavefunction or state of coherent x values. The integrand in eq. (3.3) is localized in p space by a corresponding Gaussian and so we could refer to this integrand as a state of coherent p values. The slowness variable p relates to the propagation direction of a wave and so the function $\psi^{\text{inc}}(p', x)$ (eq. 3.3) contains a spectrum of such directions windowed about p'. At high frequency a saddle-point approximation to eq. (3.3) takes the form

$$\psi^{\text{inc}}(p', x) \sim \omega^{-1} B(p', x) \exp[\mathrm{i}\omega S(p', x)] \tag{3.4}$$

and from this approximation the wavefunction $\psi^{\text{inc}}(p', x)$ will be explicitly seen to be localized in both x and p'. For this reason it may be preferable to call the form eq. (3.4) an elementary coherent state, even though it is only an approximate solution of the wave equation. This approximation will be reminiscent of a single Gaussian beam, although it does not have exactly Gaussian decay in general. Substitution of the approximation eq. (3.4) into the inverse CST (eq. 2.7) leads to a representation of the solution $u(x)$ as a sum of such beams or coherent states. The final integral approximations such as this are the object of study, because they are reasonably easy to compute once their kernels

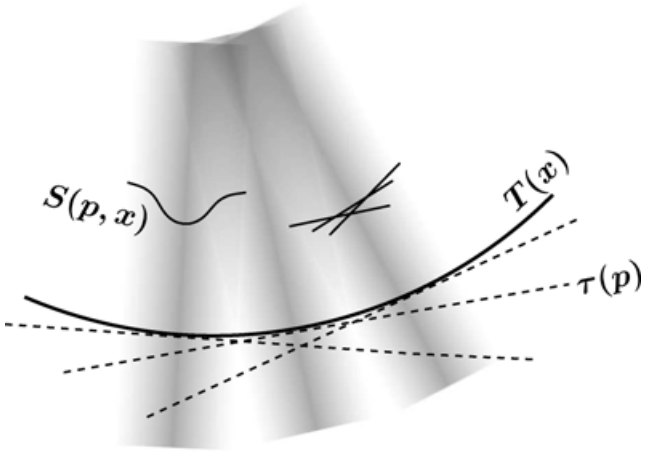

Figure 1. A depiction of the physical wave front $T(\mathbf{x}) =$ constant and its representation as the envelope of a set of tangent fronts related to $\tau(p)$, the Legendre transformation of T with respect to the lateral coordinates x at fixed z (Chapman 1978; Kendall & Thomson 1993). The wavefield associated with the physical wave front can be represented as a sum of Snell waves, each of which is associated with a single value of p and hence τ. The standard Fourier transform (or plane wave sum) describes how these partial waves are combined (e.g. eq. 3.2). Also depicted are three beams or coherent states, the summation of which is given by the inverse CST (eq. 2.7) in the text. Each CS can itself be represented as a sum of damped plane waves (e.g. eq. 3.3), depicted in the beam on the right, as a bundle of complex rays (e.g. eq. 3.10), or as a paraxial Gaussian beam carried by a real ray (e.g. eq. 3.11). The beam on the left contains a depiction of the latter involving the phase $S(p, x)$.

(eq. 3.4) are found by ray tracing in inhomogeneous media and they have desirable and flexible localization properties. Fig. 1 is an attempt to convey these ideas pictorially.

3.2 Saddle-point approximations

The high-frequency asymptotic form eq. (3.4) of ψ^{inc} in the (p', x) plane may be verified by considering the saddle-point contributions to integral eq. (3.3). Consider its phase function

$$\theta(p, p', x, x_S, z) = \mathrm{i}\big[\tau^{\text{inc}}(p, z) + p(x - x_S)\big] - \frac{1}{2\Omega}(p - p')^2, \tag{3.5}$$

now written with x rather than x' and where for once all the dependencies have been indicated on the left-hand side. The stationary point $p = p_s\,(p', x, x_S, z)$ is a solution of

$$\partial_p\theta(p)\big|_{p=p_s} = \mathrm{i}\left[\partial_p\tau^{\text{inc}}(p_s, z) + (x - x_S)\right] - \frac{1}{\Omega}(p_s - p') = 0 \tag{3.6}$$

and there are two such conditions because p is a two vector. Ostensibly p is real and in this more familiar case we recall that $\partial_p\tau^{\text{inc}}(p, z) = -X(p, z)$, the lateral range(s) traversed by a real ray of slowness p as it covers the depth range z (Chapman 1978). It follows from eq. (3.6) that whenever p' and x are related by $X(p') = x - x_S$ there is always a real stationary-phase point $p = p_s = p'$ of the integrand in eq. (3.3). The line (or subspace) $X(p') = x - x_S$ in the (p', x) plane is a special domain where the saddle-point/stationary-phase evaluation of eq. (3.3) is notable because there the decay (Ω) exponent vanishes. The points of this subspace connect each CS beam centre to a point of the physical wave front.

Now consider a point in the (p', x) plane near the special line such that $x - x_S = X(p') + \delta x$. The previous real stationary/saddle point becomes complex and we assume for now that it is close to p' by writing $p_s = p' + \delta p$. By substitution into the stationarity condition (eq. 3.6) we find

$$\delta p = -\big(\partial_p\partial_p\tau^{\text{inc}} + \mathrm{i}\Omega^{-1}\big)^{-1}\delta x + O(\delta x^2) = -\big(\partial_p\partial_p\tau^{\text{inc}} - \mathrm{i}\Omega^{-1}\big)\left(\partial_p\partial_p\tau^{\text{inc}^2} + \Omega^{-2}\right)^{-1}\delta x + O(\delta x^2), \tag{3.7}$$

where matrix $\partial_p\partial_p\tau^{\text{inc}}$ is evaluated at p' (real). Note that here and from now on it is appropriate to consider Ω to be acting as if it were a 2×2 diagonal matrix. Also, for the point-source problem under consideration we have that for p real $\partial_p\partial_p\tau^{\text{inc}} = -\partial_p X < 0$ (i.e. the real incident wave front approaching the reflector is convex downwards). Fig. 2 depicts how the saddle point may move near the real value p' as δx varies about zero, as well as possible steepest-descent paths. The latter depend on the orientation of the saddle point, which is determined from the second derivative

$$\partial_p\partial_p\theta = \mathrm{i}\big(\partial_p\partial_p\tau^{\text{inc}} + \mathrm{i}\Omega^{-1}\big). \tag{3.8}$$

Technically this should be evaluated at the complex slowness of the saddle point, but doing so at the real slowness p' is a useful approximation near the beam centre. Eqs (3.7) and (3.8) show that the question as to what is a large or small value of Ω is answered, in part, by comparison with the magnitudes of the elements or eigenvalues of the physical phase-front curvature matrix $\partial_p\partial_p\tau^{\text{inc}}$. There are three cases to consider.

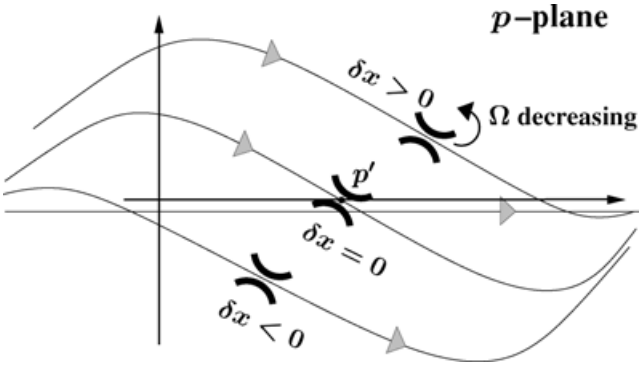

Figure 2. The saddle point of eq. (3.3) in the complex p plane. In fact we must consider this to be either the p_1 or p_2 plane. The 2-D saddle-point approximation to eq. (3.3) discussed in Section 3.2 assumes, reasonably, that the integration contours for both slowness components can be deformed independently as required. The saddle point lies on the real axis only for (p', x) on the special line and otherwise its position depends on δx approximately according to eq. (3.7). When Ω is large (as defined in Section 3.2) the saddle is oriented at almost $-\pi/4$ to the real axis and as Ω decreases it rotates to become parallel with the real axis. Thus, the original real-axis integration path deforms naturally over the saddle to give the complex-ray approximation (eq. 3.10).

(i) Case I ($\Omega\partial_p\partial_p\tau \ll 1$). In this case $\delta p \approx \mathrm{i}\Omega\,\delta x$, so considerable freedom in δx may exist if Ω is very small. From eq. (3.7) it follows that if $\delta x > 0$ then $\Im(\delta p)$ and $\Re(\delta p)$ are positive, and vice versa. Then from eq. (3.8) it follows that the saddles are oriented almost parallel to the real p-axis independently of the sign of δx, as indicated in Fig. 2. The phase at the saddle point can be reasonably approximated via

$$\theta(p_s, x) = \mathrm{i}\left[\tau^{\mathrm{inc}}(p_s, z) + p_s(x - x_S)\right] - \frac{1}{2\Omega}(p_s - p')^2$$

$$= \mathrm{i}\left[\tau^{\mathrm{inc}}(p', z) + p'(x - x_S)\right] - \mathrm{i}\frac{1}{2}\delta x\left(\partial_p\partial_p\tau^{\mathrm{inc}} + \mathrm{i}\Omega^{-1}\right)^{-1}\delta x + O(\delta x^3), \tag{3.9}$$

i.e. an expansion about p' in which eq. (3.7) has been used to replace δp with δx. This phase function indicates that the CST ψ^{inc} decays on moving away from the special line $X(p') = x - x_S$ in the (p', x) plane. The decay exponent is almost proportional to Ω, because the latter is small here, and of course ω, which is large in the asymptotic limit under consideration. Thus the overall decay away from the special line can be rapid, depending on the ratio of ω to Ω. The actual limit $\Omega = 0$ can be explained by reference to the basic definition eq. (2.4), where putting $\Omega = 0$ shows the CST to be then the standard Fourier transform plus a phase shift. Alternatively, in eq. (3.3) the case $\Omega = 0$ can be understood by noting the sharp nature of the Gaussian slowness window as this limit is approached and recalling the definition of the 1-D Dirac delta function $\delta(y) = \lim_{\epsilon\to 0}(1/2\sqrt{\pi\epsilon})\exp(-y^2/4\epsilon)$ (Gelfand & Shilov 1964 p. 37). The saddle-point approximation is therefore not actually necessary in the limit, though it gives a consistent result as the limit is approached. Overall, and in brief, when Ω is small but non-zero and the frequency ω is high, the CST ψ^{inc} is concentrated near the special line in the (p', x) plane. There is generally oscillation as well as decay and when $\Omega = 0$ the CST ψ^{inc} is in fact the usual partial or Snell wave familiar in seismology [i.e. the integrand in eq. (3.2), which is not damped].

(ii) Case II ($\Omega\partial_p\partial_p\tau \approx 1$). For intermediate Ω the saddle point is still close to p' so long as δx is small. The saddle orientation is intermediate between cases I and III, meaning it is subparallel to the real p -axis. The phase at this complex saddle point can be approximated as in eq. (3.9) above and the matrix coefficient of the quadratic δx terms can be recast using $(\partial_p\partial_p\tau^{\mathrm{inc}} + \mathrm{i}\Omega^{-1})^{-1} = (\partial_p\partial_p\tau^{\mathrm{inc}} - \mathrm{i}\Omega^{-1})\,(\partial_p\partial_p\tau^{\mathrm{inc}^2} + \Omega^2)^{-1}$. Thus, there is still exponential decay away from the special line and this is rapid when frequency ω is large.

(iii) Case III ($\Omega\partial_p\partial_p\tau \gg 1$). In this case we may still consider eqs (3.7) and (3.9) for points near the special line and conclude that there is decay away from that line. However the actual limit $\Omega \to \infty$ also deserves some discussion. To see why, consider the original definition of ψ^{inc} (eq. 2.4), which shows that for large Ω a small range of x about x' is windowed. Provided the frequency ω is high enough, we can imagine that sufficient oscillations occur within this small window to generate a wavefunction usefully described by a saddle-point approximation of eq. (3.3). Though, as $\Omega \to \infty$, the Gaussian window in eq. (2.4) (when augmented by an appropriate amplitude scaling with Ω) becomes a delta function once again and $\psi^{\mathrm{inc}}(p', x)$ becomes simply a point sample of $u^{\mathrm{inc}}(x)$. This is reflected in eq. (3.5), where for large Ω the Gaussian slowness decay term is weak in comparison with the oscillatory phase term. The stationary point of the latter alone will be real, but it will not necessarily lie near the special line in the (p', x) plane. For general x, it lies at some real $p = p_s(x)$ independent of p' as $\Omega \to \infty$. The value of the exponential decay term at this real stationary point depends on the ratio ω/Ω. If $\Omega \to \infty$ faster than ω it is unnecessary to actually take the real saddle-point approximation, as eq. (3.3) just becomes the Ω-scaled inverse Snell wave transform giving the earlier point sample of $u^{\mathrm{inc}}(x)$ and is independent of p'. If $\omega \to \infty$ faster than Ω the real saddle-point approximation from $p_s(x)$ is reasonable and is modulated by the Gaussian decay dependent on $p_s - p'$. Hence, we come to the conclusion that for large though finite Ω and high-frequency ω, the CST ψ^{inc} is still concentrated near the special line in the (p', x) plane. As $\Omega \to \infty$ it tends to $u^{\mathrm{inc}}(x)$ (to within a scaling by Ω), in which case it oscillates along x and is invariant in the direction of p'.

In order to complete the saddle-point analysis, consider the second-derivative matrix (eq. 3.8). On the special line, the real symmetric matrix $\partial_p\partial_p\tau^{\mathrm{inc}}$ has a real eigenvalue/eigenvector representation, which we write as $\partial_p\partial_p\,\tau^{\mathrm{inc}} = N\Lambda N^T$. Such a decomposition is also needed for

more general complex values of p and may be defined by analytic continuation in the neighbourhood of p'. The leading-order saddle-point result may be obtained swiftly by introducing a variable transformation (rotation) to $\bar{p} = N^T(p - p_s)$ and in terms of this variable the two steepest-descent paths away from the saddle point are defined by $\arg(\mathrm{i}(\Lambda_\alpha + \mathrm{i}\Omega^{-1})\bar{p}_\alpha^2) = \pm\pi$, for $\alpha = 1, 2$. The double integral becomes approximately two independent Gaussian integrals along the steepest-descent paths and after undoing the variable change we arrive at the leading-order 2-D saddle-point approximation to eq. (3.3) :

$$\psi^{\mathrm{inc}}(p', x) \sim \frac{1}{2\mathrm{i}\omega\Omega q_1} \frac{1}{\left(\det|\partial_p\partial_p\tau^{\mathrm{inc}} + \mathrm{i}\Omega^{-1}|\right)^{\frac{1}{2}}} \exp\left\{\mathrm{i}\omega\left[\tau^{\mathrm{inc}}(p_s, z) + p_s(x - x_S)\right] - (\omega/2\Omega)(p_s - p')^2\right\}. \tag{3.10}$$

In this expression the saddle position p_s is generally complex and the amplitude terms as well as the phase terms are evaluated at that point. The complex square root of the amplitude term is well defined by the saddle-point calculation just outlined and in more complicated problems with caustics it contains the effects of the KMAH index. This important topic in ray and Maslov theory (Červený 2001; Chapman & Drummond 1982) is handled automatically in the CS approach, but is not pursued here (see Paper I for a discussion). Formally, as $\Omega \to 0$ eq. (3.10) remains correct, as $p_s - p' = \delta p$ tends to zero like Ω. The Ω factors in the amplitude cancel and so the earlier Snell wave integrand eq. (3.2) is obtained. As $\Omega \to \infty$, however, eq. (3.10) does not tend exactly to the scaled point form of $u^{\mathrm{inc}}(x)$ discussed in case III above. Therefore, eq. (3.10) should be considered to apply only for large but finite Ω, where large means $\Omega\partial_p\partial_p\tau \gg 1$ and finite means $\omega/\Omega \gg 1$.

In the vicinity of the special line we have from eq. (3.9) the further approximation

$$\begin{aligned}\psi^{\mathrm{inc}}(p', x) \sim \frac{1}{2\mathrm{i}\omega\Omega q_1} \frac{1}{\left(\det|\partial_p\partial_p\tau^{\mathrm{inc}} + \mathrm{i}\Omega^{-1}|\right)^{\frac{1}{2}}} \exp\Bigg\{&\mathrm{i}\omega\left[\tau^{\mathrm{inc}}(p', z) + p'(x - x_S)\right] \\ &-\frac{1}{2}\mathrm{i}\omega[x - x_S - X(p')](\partial_p\partial_p\tau^{\mathrm{inc}} + \mathrm{i}\Omega^{-1})^{-1}[x - x_S - X(p')]\Bigg\}\end{aligned} \tag{3.11}$$

and now the amplitude as well as the phase are evaluated at the real slowness p'. It is this latter approximation eq. (3.11) that may interpreted as a paraxial Gaussian beam carried by a real ray and we may say this is useful for $0 \le \Omega < \infty$. The more general form eq. (3.10) requires the rays to be considered in complex position and slowness space, described next.

3.3 Phase fronts, rays and geometrical spreading

Form eq. (3.10) is actually applicable only at some distance from the point source and so for the next few paragraphs we will implicitly consider values of z somewhat removed from $z = 0$. Also, the prime on variable p will be dropped. The aim in this section is to explain the sense in which eq. (3.10) is obtainable directly as an asymptotic solution to the wave eq. (3.1) for $\psi^{\mathrm{inc}}(p, x)$. That is, as a direct complex-ray approximation for ψ^{inc}, with reference to the standard Fourier-summation form eq. (3.2) of u^{inc} or form eq. (3.3) for ψ^{inc} only in order to match with the source. Approximation eq. (3.10) is in the form eq. (3.4) with the phase function

$$S(p, x, z) = \tau^{\mathrm{inc}}(p_s, z) + p_s(x - x_S) + \frac{\mathrm{i}}{2\Omega}(p_s - p)^2, \tag{3.12}$$

where the stationary point $p_s = p_s\,(p, x, x_S, z)$ according to eq. (3.6) (with care to interpret p and p' correctly in that earlier equation). Note the z dependence has been made explicit in eq. (3.12).

For the discussion it helps to review first the three other phase functions that play roles and for brevity the superscript $^{\mathrm{inc}}$ will be temporarily omitted. Of primary importance is the phase of the physical wave front $T\,(x, z)$, defined by the real rays emanating from the source. Next comes $\tau(p, z)$, the Legendre transformation with respect to x of $T(x, z)$ (Kendall & Thomson 1993). Phase τ can be constructed either from $T(x, z)$ via the forward Legendre transformation $\tau = T - px$ or by ray tracing in (p, z) space. Such ray tracing is in fact not different from ordinary ray tracing, as it just amounts to considering the ray equations with alternative configuration- or base-space variables. The ray equations themselves are unchanged in form and there is only one set of rays, the real rays of T (Thomson & Chapman 1985 Appendix B). A third phase function is $\tau + px$, the inverse Legendre transformation appearing in the standard Fourier sum (eq. 3.2). This phase defines the Snell wave fronts (Kendall & Thomson 1993). In a homogeneous medium these Snell fronts are valid plane wave solutions of the eikonal equation and they form an envelope of the physical front $T(x, z)$ in (x, z) space. In an inhomogeneous medium the Snell waves defined by the inverse Legendre transformation $\tau + px$ for each constant p are not exact solutions of the eikonal equation in (x, z), though this does not offset the validity of the Maslov solution that uses them. It is, however, a point worth noting when comparing to the CS phase (eq. 3.12) and its associated rays. Clearly the real part of the CS phase S is closely related to the other three phases just described, and in fact on the special line in the (p, x) plane the real rays of T (and hence τ) turn out to be shared with S.

To study the evolution of phase S one substitutes eq. (3.4) into the homogeneous form of the wave equation for ψ (eq. 3.1) and observes that the leading-order term is $O(\omega^2)$. Setting the coefficient of ω^2 to zero yields an eikonal equation for $S(p, x, z)$. That is, a non-linear first-order differential equation, in general containing the derivatives $\partial_x S$, $\partial_z S$ and $\partial_p S$. For the homogeneous medium at hand, this eikonal equation is actually independent of $\partial_p S$, but more generally such a dependence arises from the PSDO $v^{-1}(x - (\mathrm{i}\omega)^{-1}\partial_p)$ mentioned just after eq. (3.1). In fact such a contribution is given by the function $v^{-1}(x - \partial_p S)$ (for an explanation see Paper I, section 4.1).

Let this CS eikonal equation be written $H^{\mathrm{CS}}(p, x, z; \partial_p S, \partial_x S, \partial_z S) = 0$. It is also helpful to introduce the familiar eikonal equation of standard ray theory $H^{\mathrm{RT}}(x, z; \partial_x T, \partial_z T) = (\nabla T)^2 - v^{-2} = 0$ and the corresponding equation in Maslov theory $H^{\mathrm{MT}}(p, z; \partial_p\tau, \partial_z\tau) = p^2 + \partial_z\tau^2 - v^{-2}(-\partial_p\tau, z) = 0$. Note that H^{RT} and H^{MT} will have the same Hamiltonian, written $H^{\mathrm{RT}}(x, z, p, q) = H^{\mathrm{MT}}(p, z, x, q)$,

leading to the same ray equations and expressing the fact that T and τ, and hence $\tau + px$, are defined by a single set of rays viewed with different variables chosen to be independent. By contrast, it turns out that in general the eikonal equation for the CS phase takes the functional form

$$H^{\mathrm{CS}}(p, x, z; \partial_p S, \partial_x S, \partial_z S) = H^{\mathrm{RT}}(x - \partial_p S, z; \partial_x S, \partial_z S). \tag{3.13}$$

The derivation of this form involves the pseudodifferential operator already mentioned and the details will be omitted (see Paper I, section 4).

The CS eikonal equation can be solved by the method of characteristics (Courant & Hilbert 1962, p. 75 and 106; Červený 2001, p. 103), though now with a 5-D configuration or base space (p, x, z) rather than the 3-D (x, z) space of standard ray theory. The CS characteristic or ray equations are in general

$$\begin{aligned} &\frac{dp}{d\nu} = \partial_{\partial_p S} H^{\mathrm{CS}} \qquad \frac{dx}{d\nu} = \partial_{\partial_x S} H^{\mathrm{CS}} \qquad \frac{dz}{d\nu} = \partial_{\partial_z S} H^{\mathrm{CS}} \\ &\frac{d(\partial_p S)}{d\nu} = -\partial_p H^{\mathrm{CS}} \quad \frac{d(\partial_x S)}{d\nu} = -\partial_x H^{\mathrm{CS}} \quad \frac{d(\partial_z S)}{d\nu} = -\partial_z H^{\mathrm{CS}} \end{aligned} \tag{3.14}$$

and the final equation for the phase is

$$\frac{dS}{d\nu} = \partial_p S \frac{dp}{d\nu} + \partial_x S \frac{dx}{d\nu} + \partial_z S \frac{dz}{d\nu}. \tag{3.15}$$

Here, ν is a parameter that increases along the rays in (p, x, z). In the laterally-homogeneous case $\partial_x H^{\mathrm{CS}} = 0$ and the fifth part of eq. (3.14) shows that $\partial_x S$ is then constant. In normal ray theory $\partial_x S$ would be indentified with lateral slowness, but here it is not to be confused with the variable p. Because we are presently dealing with a homogeneous medium, though, the variable p is also conserved along the rays, as H^{CS} is independent of $\partial_p S$ and the first part of eq. (3.14) is therefore also zero. Similarly $\partial_z S$ is conserved from the last part of eq. (3.14) in the homogeneous case. If the initial value of $\partial_z S$ is non-zero, then from the third part of eq. (3.14) and the functional form of the CS eikonal eq. (3.13) it follows that $dz/d\nu \neq 0$ along the rays. We may therefore divide the entire system of equations by $dz/d\nu$, in effect elevating z to the status of independent variable.

Thus, we come to the picture of specifying S and its derivatives in the plane (p, x) at some initial z level and tracing rays as functions of z to another level. Along these rays p, $\partial_x S$ and $\partial_z S$ are constant in the case of a homogeneous medium. Because in eqs (3.10) or (3.11) we have explicit formulae for S we can describe the initial conditions more completely. Near the special line, eq. (3.11) applies and on differentiating its phase we find that

$$\partial_x S = p - \left(\partial_p \partial_p \tau^{\mathrm{inc}} + \mathrm{i}\Omega^{-1}\right)^{-1} [x - x_S - X(p)] + O[x - x_S - X(p)]^2 \tag{3.16a}$$

$$\partial_z S = q_1 + \partial_z X \left(\partial_p \partial_p \tau^{\mathrm{inc}} + \mathrm{i}\Omega^{-1}\right)^{-1} [x - x_S - X(p)] + O[x - x_S - X(p)]^2 \tag{3.16b}$$

$$\partial_p S = x - x_S - X(p) + \partial_p X \left(\partial_p \partial_p \tau^{\mathrm{inc}} + \mathrm{i}\Omega^{-1}\right)^{-1} [x - x_S - X(p)] + O[x - x_S - X(p)]^2, \tag{3.16c}$$

where superscript $^{\mathrm{inc}}$ has been reinstated. The phase of eq. (3.10) can be used to obtain these initial momenta at points farther away from the special line, but this requires implicit differentiation of p_s using the stationarity condition (eq. 3.6) and the details will be omitted. The important point, already explicit in eq. (3.16), is that the initial momenta are complex even if the initial base-space coordinates (p_0, x_0) are real. The corresponding ray will therefore leave real (p, x) space immediately. In order for a ray to arrive at real final coordinates (p, x) at the final z level, it is in general necessary for the ray to have initially-complex values of (p_0, x_0). Thus, it is necessary to consider the initial phase (eq. 3.12) to be analytically continued to complex (p, x). However, a simplification arises because p is constant along rays (for the homogeneous medium under consideration): if the final p is real, the initial value p_0 must also be. Thus, only the initial value x_0 must be complex in our case.

The important exception to this general picture is the case of a ray emanating from a real point on the special line $x - x_S = X(p)$ in the initial z plane. For such a ray all the initial data are real and the ray remains entirely in real space. From eq. (3.12) we see that for given p the value of S is then just the value of T for a point on the physical front with standard lateral slowness p. Then from eqs (3.16a–b) we see that at constant p the derivatives $\partial_x S$ and $\partial_z S$ on the special ray become just p and q_1, respectively, and in this sense the (x, z) front associated with the real part of S at constant p is tangential to the physical front T at the point with slowness p. In other words, the CS variable p becomes coincident with the usual ray-theory momentum variable called lateral slowness for the entire special ray. However, the near neighbours of the special ray in complex (p, x) space undergo geometrical spreading that is quite different to the spreading associated with the physical front T. The approximate phase in eq. (3.11) is in fact an expansion about such a real ray. When this approximation for $\psi^{\mathrm{inc}}(p, x)$ was derived from eq. (3.10) it was not explicitly mentioned that in the latter p and x could themselves take complex values.

The geometrical spreading of the generally complex rays depends on Jacobians such as

$$J(p, x, z) = \det \left| \frac{\partial(p, x, z)}{\partial(p_0, x_0, z_0)} \right|_\nu \qquad \text{and} \qquad J'(p, x, z) = \det \left| \frac{\partial(p, x)}{\partial(p_0, x_0)} \right|_z, \tag{3.17}$$

where the latter form applies if z is taken as independent variable. These Jacobians arise when the ansatz (eq. 3.4) is substituted into the wave equation for ψ (eq. 3.1) and terms of order ω are used to derive a transport equation for the amplitude. See Paper I, section 4.5. Ostensibly, then, the spreading takes place in the higher dimensional base space (p, x) rather than just in x space as for standard ray theory or just in p space

as for Maslov theory. However, the functional form of the geometrical spreading equations derived from the CS ray equations of eq. (3.14) above leads to a reduction in the dimensionality of the determinants that are needed. The details will be omitted here and can be found in section 5 of Paper I. Suffice to say, the lower dimensional (2×2) determinant giving the amplitudes in eqs (3.10) and (3.11) is in agreement with the true geometrical spreading factors (eq. 3.17) in CS (p, x) space.

This section is concluded with comments on the point source. Although the form eq. (3.4) is not appropriate very near a point source, it can be matched with a boundary-layer (i.e. near-field) solution there and it is useful to define rays emanating from the source point itself (in the case of standard ray theory see, for example, Babič & Kirpičnikova 1979 chapter 7). These real standard rays from the source define the functions τ and X used above. The complex rays emanate from complex values of x_0 and thus the source location x_S is extended to complex space, as are τ and X. Deschamps (1971) showed that a complex source point was a convenient way to generate a Gaussian-beam wavefield from the analytic form of the homogeneous-medium Green function, and we have simply returned to his observation in a more general context.

4 REFLECTED WAVES

4.1 The standard Fourier solution and the critical-ray Weber function

The exact Fourier form of the reflected wave in $z < h$ is

$$u^{\text{refl}}(x, z) = \left(\frac{\omega}{2\pi}\right)^2 \int \frac{1}{2\mathrm{i}\omega q_1} R(p) \exp\left\{\mathrm{i}\omega\left[\tau^{\text{refl}}(p, z) + p(x - x_S)\right]\right\} dp, \tag{4.1}$$

where $\tau^{\text{refl}}(p, z) = \int_0^h - \int_h^z q_1(p)dz$ is the accumulated vertical phase. The plane wave reflection coefficient is

$$R(p) = \frac{q_1 - q_2}{q_1 + q_2}, \tag{4.2}$$

where $q_2 = (v_2^{-2} - p^2)^{\frac{1}{2}}$ is the positive downgoing slowness in the lower layer. In order to analyse eq. (4.1) and its CST it is necessary to consider the effects of the scalar lateral range from the source and we assume for simplicity that this corresponds to the direction $x_1 (>0)$. The orthogonal lateral direction x_2 and the corresponding p_2 integration in eq. (4.1) contribute geometrical spreading factors to the response, but the complications associated with the critical angle arise essentially via the single slowness integration along p_1. Subsequent integration over p_2 builds the three-dimensionality and only a limited range of values around $p_2 = 0$ is asymptotically important when $x_2 - x_{2S} = 0$. An alternative approach would be to perform the p_2 integration first by the stationary-phase method, but the preference here is to leave the p_2 integration undone and focus on the effects of range on the p_1 integral.

It is well known that when $v_2 > v_1$ and $x_1 > 0$ the reflection response has a ray contribution from a stationary point with respect to p_1 of the phase in eq. (4.1) plus a possible head wave contribution from the algebraic amplitude singularity at the real branch point of q_2 at $p_1 = p_c = (v_2^{-2} - p_2^2)^{\frac{1}{2}} > 0$. The original path of integration along the real p_1 -axis can be used to find the leading-order behaviour of each of these signals separately: see Chapman (1978) for a time-domain first-motion analysis and Thomson & Chapman (1986) for the corresponding real-axis frequency-domain analysis. It is, however, more common to use complex p_1 contours passing over the saddle point and around the branch point, as explained in the caption to Fig. 3 (see also Brekhovskikh 1980, figs 28.1 and 30.1; Aki & Richards 2002, figs 6.6 and 6.9). The mathematical necessity of a distinct head wave is more readily appreciated when it can be associated with a distinct branch-cut integral arising only in the post-critical region. It is somewhat more difficult to visualize why a head wave must occur for post-critical receivers and not pre-critical ones when using only the original real-axis oscillatory integral. This is because it depends on the differing cancellations of peaks and troughs as the receiver position changes. However, it can be done and for the isolated real-axis branch-point contribution see the expressions in Thomson & Chapman (1986, case i, p. 291).

The x_1 critical distance at level z is denoted $X_c = X_1(p_c) = -\partial_{p_1}\tau^{\text{refl}}$, a function of p_2 note. For receivers in this vicinity of the x_1-axis (recall $x_2 - x_{2S} = 0$) the p_1 saddle point and branch point are close in comparison with the saddle width or Fresnel zone. In this case the uniformly valid asymptotic form of the response takes a canonical form involving the Weber function (Bleistein 1966; Bleistein & Handelsman 1986, section 9.4; Brekhovskikh 1980, p. 271). As preparation for the corresponding CST result, a summary description of this asymptotic form for the standard reflection expression (eq. 4.1) is given here and in Appendix A. The leading-order behaviour can be broadly understood by approximating the phase in eq. (4.1) according to

$$\tau^{\text{refl}} + p(x - x_S) = \tau^{\text{refl}}(p_c, p_2, z) + p_c(x_1 - x_{1S}) + p_2(x_2 - x_{2S}) + a(p_1 - p_c) + \frac{1}{2}b(p_1 - p_c)^2 + O(p_1 - p_c)^3, \tag{4.3}$$

where $a = x_1 - x_{1S} - X_c$ and $b = \partial_{p_1}^2\tau^{\text{refl}} = -\partial_{p_1}X_1|_{p_c} < 0$. Note that p_c, a and b all depend on p_2, though by the symmetry only weakly (i.e. to second order) at $p_2 = 0$. Technically, rather than using the first few terms of a Taylor series as implied by eq. (4.3), one ought to define a stretching of the p_1-axis to put the phase exactly into the quadratic canonical form throughout a finite neighbourhood of p_1 near p_c (Bleistein 1966). However, we may reasonably assume $\partial_{p_1}X_1$ is slowly varying near p_c and the quadratic approximation indicated by eq. (4.3) will suffice for the present purposes, at least in a boundary layer around the critically-reflected ray. Note that a may be positive (post-critical) or negative (pre-critical). The reflection coefficient may be represented in a p_1 neighbourhood of the critical slowness p_c by the expression

$$R(p_1) = r_1(p_1) + r_2(p_1)(p_c - p_1)^{\frac{1}{2}}, \tag{4.4}$$

where r_1 and r_2 are again smooth functions of p_1 (as well as p_2 and p_c).

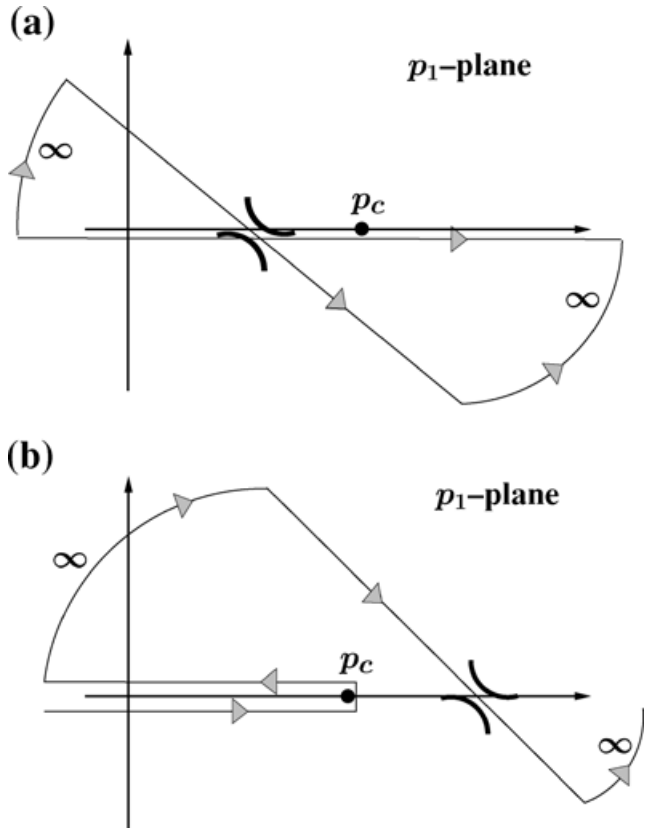

Figure 3. Contours for the asymptotic evaluation of the standard Fourier plane wave summation form of the reflected wave (eq. 4.1). For definiteness we may consider the original contour of p_1 integration to be infinitesimally below the real axis. The sign of q_2 is positive real or positive imaginary on this contour, corresponding to downgoing waves in the lower half space. (a) In the pre-critical region the original real-axis path of the p_1 integration can be deformed over the saddle point without encircling the branch point p_c. (b) In the post-critical region, deformation of the contour over the saddle requires an excursion around the branch point if the integral is to remain unchanged. When the saddle and branch point are sufficiently isolated, the former gives the post-critical or total reflection, with a complex plane wave reflection coefficient, and the two-sided branch-line integral has a leading-order contribution from the vicinity of p_c giving the head wave.

The leading term in $R(p_1)$ (eq. 4.4) contributes just a standard p_1 stationary-phase contribution to u^{refl}. The second term contributes the branch point and its form is described in relation to the Weber function in Appendix A. The result is that around the critically-reflected ray the contribution to u^{refl} from the second term in eq. (4.4) has the asymptotic form

$$u^{\text{refl}}_{r_2}(x,z) \sim \left(\frac{\omega}{2\pi}\right)^2 \int \frac{1}{2\mathrm{i}\omega q_1} r_2 \mathrm{Cr}(a,b,\omega) \exp\left\{\mathrm{i}\omega\left[\tau^{\text{refl}}(p_c,p_2,z) + p_c(x_1 - x_{1S}) + p_2(x_2 - x_{2S})\right]\right\} dp_2, \tag{4.5}$$

where $x_2 - x_{2S}$ has been retained for clarity and because approximation eq. (4.5) may in fact be useful if $x_2 - x_{2S} \approx 0$. The new critical-incidence function $\mathrm{Cr}(a, b, \omega)$ contains the Weber function and is defined in Appendix A. This function describes the essential behaviour when the saddle-point and branch-point cannot be treated in isolation, with parameter a controlling the distance from the critically-reflected ray and parameters b and ω controlling the width of the transition region or boundary layer around that ray.

As the coefficients a and b, and p_c itself, vary slowly near $p_2 = 0$ a further leading-order asymptotic analysis of eq. (4.5) essentially reduces to a stationary-phase evaluation of the oscillatory p_2 integral with an amplitude term containing the Weber function. The result is the same as that which would have occurred via the alternative route of taking the p_2 integral first and studying the p_1 integral second.

4.2 The CST $\psi^{\text{refl}}(\boldsymbol{p}, x)$

The CST of the reflected wave is obtained by applying eqs (2.4) or (2.5) to eq. (4.1), changing the order of integration and performing the integration with respect to x. This yields

$$\psi^{\text{refl}}(p',x) = \left(\frac{2\pi}{\omega\Omega}\right)\left(\frac{\omega}{2\pi}\right)^2 \int \frac{1}{2\mathrm{i}\omega q_1} R(p) \exp\left\{\mathrm{i}\omega\left[\tau^{\text{refl}}(p,z) + p(x - x_S)\right] - (\omega/2\Omega)(p - p')^2\right\} dp. \tag{4.6}$$

Eq. (4.6) shows that this wavefield CST can be thought of as a spectrum of damped plane waves parameterized by p, just as for the incident wave (eq. 3.3). As for the latter, applying the inverse CST (eq. 2.7) to eq. (4.6) returns $u^{\text{refl}}(x, z)$ (eq. 4.1) straightforwardly, as the p' integral separates. The CST (eq. 4.6) contains all the information required to describe the head wave and critical-ray waveforms exactly, and this should carry through to the high-frequency local approximations.

The next step, therefore, is to reduce eq. (4.6) to the same form as eq. (3.4), facilitating a simplified ray interpretation. A saddle-point evaluation is again relevant, but now there is also the branch point in $R(p)$ to consider.

4.3 Saddle-point contributions to $\psi^{\text{refl}}(p, x)$: complex and real reflected rays and reflected paraxial beams

Assume for now that the reflection coefficient is smooth. Then as far as integral eq. (4.6) is concerned the situation follows closely that for the incident wave in Section 3.2. When p' and x are related by $X(p') = -\partial_p \tau^{\text{refl}} = x - x_S$ the stationary point of the complex phase in eq. (4.6) lies at a real value $p = p_s = p'$. The phase of the saddle-point approximation is then real, though the amplitude is complex. More generally the saddle position p_s is complex and when p' and x are close to the special line the analogue of eq. (3.7) for τ^{refl} may be used to study how the saddle moves. Because $R(p)$ is smooth by assumption the two steepest-descent paths are reached without complication and one finds

$$\psi^{\text{refl}}(p', x) \sim \frac{1}{2\mathrm{i}\omega\Omega q_1} \frac{R(p_s)}{\left(\det|\partial_p\partial_p\tau^{\text{refl}} + \mathrm{i}\Omega^{-1}|\right)^{\frac{1}{2}}} \exp\left\{\mathrm{i}\omega\left[\tau^{\text{refl}}(p_s, z) + p_s(x - x_S)\right] - (\omega/2\Omega)(p_s - p')^2\right\}. \tag{4.7}$$

This expression can again be interpreted in terms of complex rays, but now there is an important constraint. The depth $z = h$ of the interface is a real variable. If the ray equations are implemented in their basic form (eq. 3.14) with ν as an independent path variable, then that variable must assume complex values in order for the ray to reflect at the real value $z = h$. An aspect of complex rays that was not discussed earlier is the fact that the path variable ν is not unique for given ray endpoints, or in this case a given intermediate point. For a discussion of this see Thomson (1997). If the ray equations are implemented with z as independent variable, as can be done for this homogeneous-medium example, then it is automatic that the source, reflector and receiver z values are all real. However, the lateral position x at which each complex ray constituting the CS impinges upon the reflector is in general complex whichever ray tracing scheme is used.

For values of p' and x near the CS centre or axis, an expansion about the corresponding special real ray is again possible. Approximating the reflection coefficient by its value at p' we find

$$\psi^{\text{refl}}(p', x) \sim \frac{1}{2\mathrm{i}\omega\Omega q_1} \frac{R(p')}{\left(\det|\partial_p\partial_p\tau^{\text{refl}} + \mathrm{i}\Omega^{-1}|\right)^{\frac{1}{2}}} \exp\left\{\mathrm{i}\omega\left[\tau^{\text{refl}}(p', z) + p'(x - x_S)\right]\right.$$
$$\left. -\frac{1}{2}\mathrm{i}\omega[x - x_S - X(p')]\left(\partial_p\partial_p\tau^{\text{refl}} + \mathrm{i}\Omega^{-1}\right)^{-1}[x - x_S - X(p')]\right\}. \tag{4.8}$$

These formulae describe the pre- or post-critical CS reflection given by the real or complex rays and as for the corresponding results at the end of Section 3.2 they may be used when $0 \le \Omega < \infty$. An important point is that even for the most local approximation (eq. 4.8) the reflection coefficient may be complex and this constitutes an additional phase contribution for each beam. Brekhovskikh (1980, p. 101) presents a model of a beam as a sum of plane waves that similarly captures the importance of the post-critical reflection coefficient and explains experimental observations of beam shifts on reflection. In the present context, the more general CS or beam form (eq. 4.7) has a complex reflection coefficient even in the so-called pre-critical region, in view of the generally-complex stationary point p_s and rays.

4.4 Isolated branch-point contributions to $\psi^{\text{refl}}(p, x)$ when $\Omega \neq 0$: peripherally-diffracted beams

For definiteness and as in Section 4.1 for the standard Fourier solution, we consider propagation along the x_1-axis by choosing $x_2 - x_{2S} = 0$. Again there is the practical choice of performing first either the p_2 or the p_1 integration. The latter will also be chosen here and the p_2 integration will again be left undone. So long as p_2 remains real the branch point remains at a real $p_1 = p_c$. The reflection-coefficient representation eq. (4.4) still applies and once more the leading (analytic) term gives rise to a standard saddle-point approximation like eqs (4.7) or (4.8) above, with $r_1(p)$ replacing $R(p)$.

Ignoring for now the outer p_2 integration, the branch-point contribution to eq. (4.6) rests on the key p_1 integral

$$I_{r_2}(p_1', p_2, x_1 - x_{1S}, z, \omega) = \int \frac{1}{2\mathrm{i}\omega q_1} r_2(p_1)(p_c - p_1)^{\frac{1}{2}} \exp\left\{\mathrm{i}\omega\left[\tau^{\text{refl}}(p, z)\right.\right.$$
$$\left.\left. + p_1(x_1 - x_{1S})\right] - (\omega/2\Omega)(p_1 - p_1')^2\right\} dp_1. \tag{4.9}$$

As $\Omega \to 0$ the integrand here [when combined with an exterior factor of Ω in eq. (4.6)] acquires the delta function $\delta(p_1 - p_1')$. In this case the integral (eq. 4.9) collapses and the branch point is transferred exactly into ψ^{refl} and hence the inverse CST (eq. 2.7). This is equivalent to the standard Fourier case. In contrast, the description to be given below assumes that $\Omega \neq 0$, in which case the CS beams of finite width may be analysed in terms of individual saddle- and branch-point signals.

We may attempt to study the isolated branch-point contribution to eq. (4.9) in the same real-axis manner as Thomson & Chapman (1986; these authors used the method of Laplace, as described by Bender & Orszag 1999). A starting point is an expansion of the phase in eq. (4.9) in powers of p_1 about p_c:

$$\mathrm{i}\left[\tau^{\text{refl}}(p, z) + p_1(x_1 - x_{1S})\right] - \tfrac{1}{2\Omega}(p_1 - p_1')^2 = \mathrm{i}\left[\tau^{\text{refl}}(p_c, p_2, z) + p_c(x_1 - x_{1S})\right.$$
$$\left. + a(p_1 - p_c) + \tfrac{1}{2}b(p_1 - p_c)^2\right] - \tfrac{1}{2}\Omega^{-1}(p_c - p_1')^2 + O(p_1 - p_c)^3, \tag{4.10}$$

where now $a = x_1 - x_{1S} - X_c + \mathrm{i}\Omega^{-1}(p_c - p_1')$ and $b = \partial_{p_1}^2\tau^{\text{refl}} + \mathrm{i}\Omega^{-1}$ are complex. When $x_1 - x_{1S} - X_c$ is far from zero the saddle point of the last section is far removed and it is tempting to assume that the linear $a(p_1 - p_c)$ term in the phase is locally dominant around p_c. This

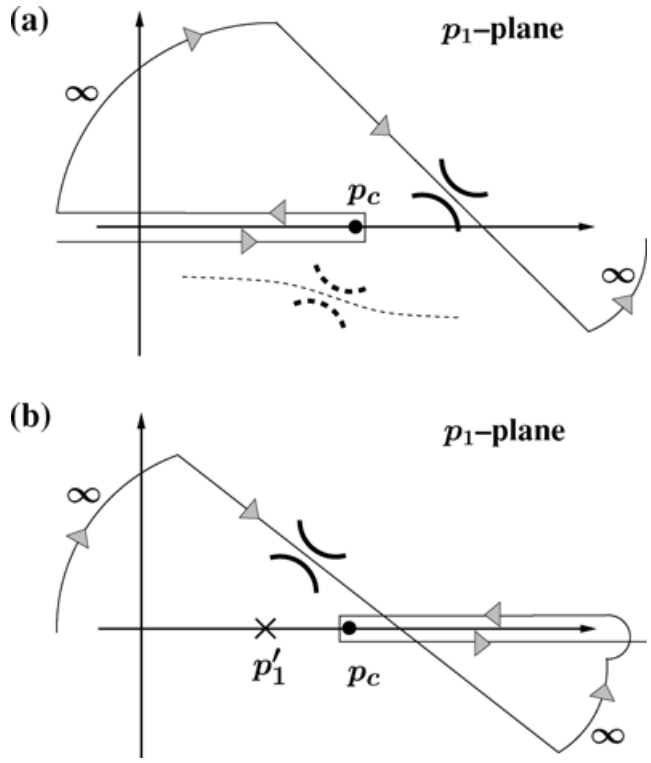

Figure 4. Possible p_1 contours equivalent to the real-axis integration defining integral (eq. 4.9). Once again the original contour may be envisaged as running infinitesimally below the real axis. (a) A case where the central ray of the CS beam is incident beyond the critical angle ($p_1' > p_c$). The p_1 saddle (solid) lies above the real axis, corresponding to $\delta x_1 > 0$ in the analogue of eq. (3.7). In other words, the observation point is at the leading or wider-incidence-angle edge of the CS beam (Fig. 5a) and the saddle point contributes an appropriately damped signal given by a reflected complex ray. Deforming the contour over the saddle point introduces a two-sided branch-line integral giving a head wave type contribution in a fashion similar to the standard Fourier case of Fig. 3(b). The contributing slownesses just less than p_c correspond to plane wave constituents of the CS beam that are arriving near the critical angle. These are located within the trailing-edge or narrower-angle periphery of the reflected beam and they generate a damped head wave because they themselves are damped. In contrast, the dashed saddle point and integration path indicate another possibility that $\delta x_1 < 0$ in the analogue of eq. (3.7), meaning that the observer is in the trailing edge of the reflected beam and local plane wave constituents are not quite at the critical angle. Although a branch-cut integral is not required, the saddle point may still be influenced by the branch point, unless Ω is very small and the saddle is very compact (Section 3, case I; Section 4.4). (b) Even if the central ray of the incident CS beam is pre-critical ($p_1' < p_c$) it is conceivable that some plane wave components at the leading edge ($\delta x_1 > 0$) are beyond the critical angle (Fig. 5b). In order to collect a localized branch-point signal the branch-line integral must be taken towards the right as indicated, in order to ensure decay as a result of the linear $a(p_1 - p_c)$ term in eq. (4.10). Again, however, the proximity of the branch point and the steepest-descent path suggests they interfere. If they do not, the branch-point head wave signal is exponentially damped.

runs into difficulty, though, because on one side or the other of the branch point the imaginary part of coefficient a will contribute a term that grows exponentially with $p_1 - p_c$, the direction of growth depending on the sign of $p_c - p_1'$. The total phase, including all the quadratic terms in p_1, certainly guarantees decay in both directions away from p_1' (rather than p_c), so the difficulty is more apparent than real.

It is questionable that an isolated branch-point contribution can be obtained from a straightforward real-axis local analysis and so complex contours are considered. The saddle point passes either above or below the branch point in the complex p_1 plane, depending on whether δx_1 in the analogue of eq. (3.7) is positive or negative (i.e. depending on which side of the beam centre or (p', x) special line the observation point lies). The varying orientation of the saddle according to the value of Ω also affects the level of its interaction with the branch point. Figs 4 and 5 and their captions describe representative situations. An overall conclusion (Fig. 4a) is that when p_1' is sufficiently greater than p_c, the contour deformation required to collect an isolated post-critical saddle-point signal still requires a two-sided branch-cut integral analogous to that used in the standard Fourier representation of Section 4.1. In this case ($p_1' > p_c$) the linear $a(p_1 - p_c)$ term in the phase (eq. 4.10) does cause decay to the left of p_c and an isolated head wave signal can then be inferred from the neighbourhood of that point. Details can be found in Appendix B. Note that the magnitude of this diffracted signal is exponentially damped according to the magnitude of $p_c - p_1'$, which is large as the saddle point is by assumption well removed.

Fig. 4(a) also shows an alternative scenario (broken lines) in which the saddle position and orientation conspire to make the branch point avoidable even when p_1' is ostensibly close to or larger than p_c. This case corresponds to a position within the trailing edge of the beam, where the local constituent plane wave has not reached the critical angle even though the central plane wave has.

Still another situation is depicted in Fig. 4(b). In this case the complex saddle is situated above and to the left of p_c, signifying that the incident beam is mainly pre-critical and the observer is placed towards the leading edge of the reflected beam [i.e. $\delta x_1 > 0$ in the analogue of eq. (3.7)]. To avoid encircling the branch point when collecting the reflection saddle-point contribution, a two-sided branch-cut integral

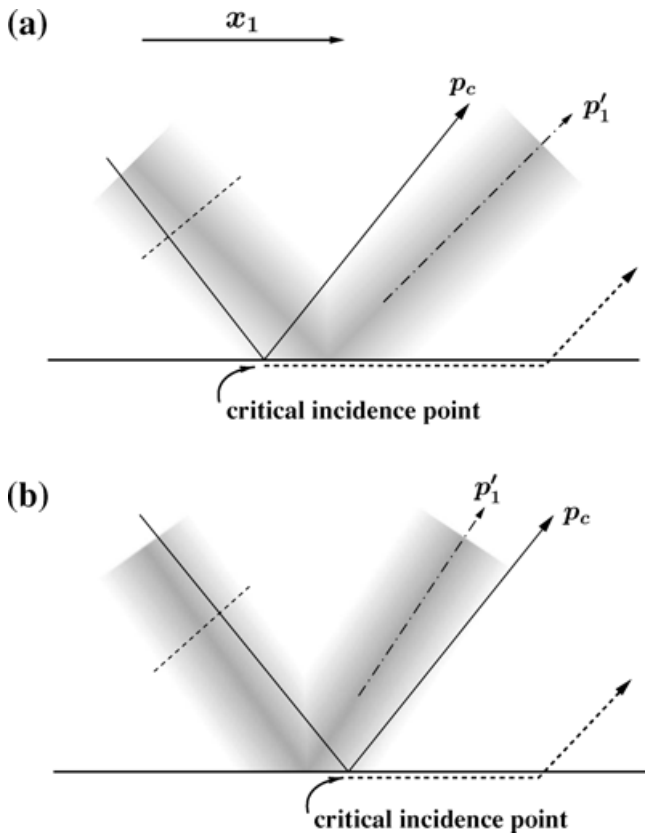

Figure 5. Depictions of reflected CS beams in the (x_1, z) plane. (a) A beam for which the real central ray with slowness p_1' is incident beyond the critical angle (or slowness p_c). The dashed diffracted ray carries a head wave type arrival excited by those plane wave components in the incident beam that are just pre-critical. A representative plane wave component is shown by the dashed front in the incident beam. (b) A beam for which the real central ray arrives at less than the critical angle. Some plane wave components (dashed) have larger slowness and generate a diffracted signal.

is required, this time to the right of p_c. The linear term $a(p_1 - p_c)$ decays to the right in this case ($p_1' < p_c$). Though the beam centre and its environs are pre-critical, some plane wave components at the leading edge are at the critical angle and beyond. They correspond to the neighbourhood $p_1 \geq p_c$ and again a head wave damped according to $p_1' - p_c$ is contributed (see Appendix B). Arguably, the scenarios of these last two paragraphs are significant only when the saddle point and branch point are in reasonably close proximity, in view of the damping. However, even such damped head waves are technically required later (Section 4.6).

Lastly, we must consider the dependence on the remaining slowness integration variable p_2. We know that if (p_2', x_2) is not on the special line the pure saddle-point result of section Section 4.3 involves a complex stationary point, indicating for example that the observer is displaced to one side or the other of the vertical propagation plane of the CS real central ray. This suggests that if the remaining p_2 integration in eq. (4.11) below is to be approximated by a p_2 saddle-point contribution, then complex p_2 values should be accommodated in the present section. The consequence for this section is that the p_1 branch point becomes complex. However, the interplay between saddle points and the branch point remains qualitatively similar. Intuitively, we would expect the isolated branch-point contribution to decay also as the vertical plane of the central ray is distanced, meaning geometrically that the head wave excited by the beam will be focussed around this vertical plane as well as weakening away from the main reflected beam within the vertical plane.

4.5 Uniformly-asymptotic form of $\psi^{\text{refl}}(p, x)$ around the critically-reflected ray ($\Omega \neq 0$)

Even though the coefficients a and b in expansion eq. (4.10) are complex, the essential geometrical properties of the key integral (eq. 4.9) conform with those discussed for the Weber-function representation in Section 4.1 and Appendix A. The conclusion, therefore, is that the function $\mathrm{Cr}(a, b, \omega)$ only requires analytic continuation of its first two arguments in order to describe the $r_2(p)$ contribution to the CS around a critically-reflected real central ray. Reinstating the p_2 integration gives

$$\psi^{\text{refl}}_{r_2}(p', x) = \left(\frac{2\pi}{\omega\Omega}\right)\left(\frac{\omega}{2\pi}\right)^2 \exp\left[-(\omega/2\Omega)(p_c - p_1')^2\right] \int \frac{1}{2\mathrm{i}\omega q_1} r_2 \mathrm{Cr}(a, b, \omega)$$
$$\exp\left\{\mathrm{i}\omega\left[\tau^{\text{refl}}(p_c, p_2, z) + p_c(x_1 - x_{1S}) + p_2(x_2 - x_{2S})\right] - (\omega/2\Omega)(p_2 - p_2')^2\right\}\, dp_2. \tag{4.11}$$

Note that $x_2 - x_{2S}$ has been included for clarity, because we may reasonably consider eq. (4.11) under the weaker condition $x_2 - x_{2S} \approx 0$.

As the observer moves away from the critically-reflected real ray in the (x_1, z) plane the function $\mathrm{Cr}(a, b, \omega)$ displays separate contributions from its saddle point and branch point (just like the original integral described in Sections 4.3 and 4.4). The former describes the reflected CS beam around the critical ray, but loses accuracy on moving away as a result of the quadratic approximation in the phase. That is, it matches with the saddle-point signals of Section 4.3 only at the edges of the critical-ray boundary layer. The separated branch-point signal centred on p_c actually remains valid in form as the observer moves further into the post-critical region (Appendix B). This is a consequence of the lateral homogeneity. Because eq. (4.11) is to be used for values of p_1' around p_c, it is seen that the exponential decay term before the integral will be of order unity and so these separated branch-point signals are only weakly damped. They will constitute the main contributions to the final head wave in the post-critical region (Section 4.6; Appendix B).

The next step might be to approximate the p_2 integral by exploiting the weak dependence of the coefficients a and b around $p_2 = 0$, which remains true even when they are complex. A new situation arises compared to the standard Fourier case, though, because even if $x_2 - x_{2S} = 0$, $p_2 = 0$ is an exact stationary-phase value for the exponential phase term shown in eq. (4.11) only when p_2' and x_2 are related by the special condition $X_2(p_2') = -\partial_{p_2}\tau^{\mathrm{refl}} = x_2 - x_{2S}$. For more general values of p_2' and x_2, the stationary-phase value of $p_2 \neq 0$ may be estimated from the analogue of eq. (3.7) for τ^{refl}. Geometrically, given $x_2 - x_{2S} = 0$ the choice of $p_2' \neq 0$ amounts to selecting a CS beam that is propagating at an angle to the (x_1, z) vertical plane and calculating its contribution within that plane. Because in general this stationary value of p_2 is complex, the branch-point considerations of the last section (Section 4.4) must also be extended to that case and they do so straightforwardly as indicated at the end of that section.

4.6 Synthesis or coherent-state summation ($\Omega \neq 0$)

The final step is to substitute $\psi^{\mathrm{refl}}(p', x)$ from eq. (4.6) or its approximations into the inverse CST (eq. 2.7). Recall that integration over p' (real) corresponds to summation over all the CS beams contributing at the observation point x. Also, the case $\Omega = 0$ has been separately considered just after eq. (4.9). Later expressions, exemplified by eq. (4.11), utilize expansion (eq. 4.10) and the factoring of the quadratic Ω-dependent phase terms there represents a potential pitfall for discussions involving the delta-function limit.

When p' is far from the critical slowness, the corresponding reflected CS contributes asymptotically a bundle of complex rays (eq. 4.7) or a paraxial Gaussian beam (eq. 4.8) to the response at x. The synthesis integral (eq. 2.7) does in fact depend on Ω in view of the approximate nature of the integrand in these cases, however this dependence is expected to be weak. For example, a saddle-point evaluation of eq. (2.7) with these integrands can be shown to agree with standard ray theory for the reflection. This rests on how the second derivatives of the complex phase combine with the complex amplitude to give the standard real geometrical spreading function, as outlined in Appendix C of Paper I. The CS synthesis or summation is an alternative to the standard ray approximation, which remains asymptotically valid in more complicated situations involving caustics and pseudocaustics. The ability to vary Ω is an attractive feature as it amounts to a testing parameter for the approximations. If dependence on Ω is significant the results should be considered suspect.

In order to describe the critical-ray and branch-point contributions to the synthesis integral (eq. 2.7), we again focus on the p_1' integration for receivers along x_1. The important contributions are somewhat imperfectly described as being of two types. For an observation point far from from the critical distance, each CS beam in eq. (2.7) contributes either an isolated branch-point signal of Section 4.4 or a branch-point signal from the function $\mathrm{Cr}(a, b, \omega)$ in eq. (4.11), as described in Section 4.5. These two contribution types turn out to be functionally the same (Appendix B) and although they are individually damped according to $\exp[-(\omega/\Omega)(p_c - p_1')^2]$ the integration with respect to p_1' ensures their collective effect will be the head wave. It might also be noted here that the non-exponential amplitude factors of the individual CS branch-point signals are Ω dependent, but as with the saddle-point contributions of the last paragraph the integrated response is expected to be only weakly dependent on Ω. This is discussed at the end of Appendix B.

When the observation point itself is close to the critical distance, the uniformly asymptotic form (eq. 4.11) must assume primary importance. Variable p_1' appears outside the integral in eq. (4.11) and also within the special function $\mathrm{Cr}(a, b, \omega)$ via its argument a. Further analysis may yield an analytic form for the p_1' integral with such an integrand, but in its absence numerical integration will be required. In other words, the integration of the Weber functions does not appear to reduce to a single Weber-function expression as obtained by the standard Fourier method. It is once again a different, though equally valid, asymptotic representation.

Lastly, the observations of this section can be seen in the light of the Fourier uncertainty principle (Kaiser 1994, p. 52). In the standard Fourier representation the head wave comes from a point singularity p_c in the transformed or p_1' domain. The CST localizes in the x domain and as one would expect from the uncertainty relation there is a corresponding spreading out of the head wave contributions in the p_1' domain. For the analytic problem at hand there is no tangible benefit from this broadening of the contributions and it simply complicates matters. By contrast, a pseudocaustic can also be called a slowness-domain point singularity and for that problem the smoothing is appropriate and, in fact, it leads to an asymptotically valid solution where otherwise (i.e. for $\Omega = 0$) it would be invalid.

5 CONCLUDING REMARKS

A long-standing question about the description of pure head waves by the Gaussian-beam method (Červený 1985; White *et al.* 1987; Weber 1988; Nowack 2003) has essentially been answered using the exact forward and inverse coherent-state transform. However, resolving this idealized theoretical issue is not the ultimate goal here. The real purpose of this paper is to help establish the coherent-state transform as a useful extension of the Fourier transform in all those areas of seismology where plane wave decomposition and synthesis are tools. The

forward coherent-state transform shows how initial data, either modelled or recorded seismograms, should be decomposed and how analysis of the wave equation under this transform is then needed in order to understand how the localized, yet overlapping, signals or beams propagate. In this paper, an attempt has been made to explain the propagation stage by using a known analytic solution for homogeneous layers. However, this approach does not fully explain how a ray approximation can be obtained from the coherent-state transform of the wave equation in a continuously variable medium. That would require the use of pseudodifferential operators and it has a rather long derivation culminating in the geometrical spreading calculation. Despite the conceptual and algebraic steps involved, though, the final ray expressions that one would implement take the same form as the more rapidly derived formulae presented here. The reader is referred to Paper I for the anisotropic elastic case.

The real-ray approximations of eqs (3.11) and (4.8) have been referred to as paraxial Gaussian beams, but note that the derivations here and in Paper I do not use ray-centered coordinates as in the original Gaussian-beam literature. The distinction is made even more clear when one considers that the coherent-state rays are to be understood in a higher-dimensional space and that the geometrical spreading idea extends naturally to this complex space giving the CS amplitude. The technically exact form of the inverse CST suggests that the relative contributions of individual CS beams expressed in the global coordinate frame are subject to less uncertainty than would be those of standard Gaussian beams using each axial ray-centered coordinate to locate the receiver.

A benefit of the coherent-state approach is the systematic way it removes the caustic singularities besetting ray and Maslov theory, and also the endpoint signals affecting the latter. For a numerical example see Paper I. There should be significant freedom in the choice of parameter Ω defining the beams. This flexibility is an attractive feature not only for modelling, but also for the processing of finite and noisy data sets. For example, the coherent-state method should provide a robust and rapid asymptotic waveform for diffraction tomography and related techniques (Burridge *et al.* 1998; Dahlen *et al.* 2000; Nolet *et al.* 2003; Baig *et al.* 2003). Using conventional ray theory for the reference-medium Green function in these Born waveform techniques precludes the possibility that subtle or even not-so-subtle (i.e. caustic) waveform variations occur in that reference medium. Such variations may arise even preceding wave front metamorphosis or folding as a result of caustics and a less-local technique integrating over a bundle of rays is an asymptotic solution.

ACKNOWLEDGMENTS

The author is grateful to the anonymous reviewers and one in particular for suggesting helpful wording changes. This work was supported by an NSERC Individual Research grant.

REFERENCES

Abramowitz, M. & Stegun, I.A., 1965. *Handbook of mathematical functions,* Dover Publications, Inc., New York.

Aki, K. & Richards, P.G., 2002. *Quantitative Seismology,* Univ. Science Books, Sausalito.

Babič, V.M. & Kirpičnikova, N.Y., 1979. *The boundary-layer method in diffraction problems,* Springer-Verlag, Berlin.

Baig, A.M., Dahlen, F.A. & Hung, S.-H., 2003. Traveltimes of waves in three-dimensional random media, *Geophys. J. Int.,* **153,** 467–482.

Bender, C.M. & Orszag, S.A., 1999. *Advanced mathematical methods for scientists and engineers,* Springer-Verlag, New York.

Bleistein, N., 1966. Uniform asymptotic expansions of integrals with stationary point near algebraic singularity, *Comm. Pure Appl. Math.,* **19,** 353–370.

Bleistein, N. & Handelsman, R.A., 1986. *Asymptotic expansions of integrals,* Dover Publications, Inc., New York.

Brekhovskikh, L.M., 1980. Waves in layered media, Academic Press, Orlando.

Burridge, R., de Hoop, M.V., Miller, D. & Spencer, C.P., 1998. Multiparameter inversion in anisotropic elastic media, *Geophys. J. Int.,* **134,** 757–777.

Červený, V., 1985. Gaussian beam synthetic seismograms, *J. Geophys.,* **58,** 44–72.

Červený, V., 2001. Seismic ray theory,Cambridge Univ. Press, London.

Červený, V. & Ravindra, R., 1971. *Theory of seismic head waves,* Univ. of Toronto Press, Toronto.

Červený, V., Popov, M.M. & Pšenčík, I., 1982. Computation of wavefields in inhomogeneous media—Gaussian beam approach, *Geophys. J. R. astr. Soc.,* **70,** 109–128.

Chapman, C.H., 1978. A new method of computing synthetic seismograms, *Geophys. J. R. astr. Soc.,* **54,** 481–518.

Chapman, C.H. & Drummond, R., 1982. Body-wave seismograms in inhomogeneous media using Maslov asymptotic theory, *Bull. seism. Soc. Am.,* **72,** S277–S317.

Courant, R. & Hilbert, D., 1962. *Methods of mathematical physics,* Wiley Interscience Publishers, New York.

Dahlen, F.A., Hung, S.-H. & Nolet, G., 2000. Fréchet kernels for finite-frequency traveltimes-I. theory, *Geophys. J. Int.,* **141,** 157–174.

Deschamps, G.A., 1971. Gaussian beam as a bundle of complex rays, *Electronics Letters,* **7,** 684–685.

Foster, D.J. & Huang, J.-I., 1991. Global asymptotic solutions of the wave equation, *Geophys. J. Int.,* **105,** 163–171.

Gelfand, I.M. & Shilov, G.E., 1964. *Generalized functions,* Academic Press, New York.

Hill, N.R., 2001. Prestack Gaussian-beam depth migration, *Geophysics,* **66,** 1240–1250.

Jeffreys, H. & Jeffreys, B., 1980. *Methods of mathematical physics,* Cambridge Univ. Press, Cambridge.

Kaiser, G., 1994. *A friendly guide to wavelets,* Birkhäuser, Boston.

Keilis-Borok, V.I., 1989. *Seismic surface waves in a laterally inhomogeneous Earth,* Kluwer Academic Publishers, Dordrecht.

Kendall, J.-M. & Thomson, C.J., 1993. Maslov ray summation, pseudocaustics, Lagrangian equivalence and transient seismic waveforms, *Geophys. J. Int.,* **113,** 186–214.

Klauder, J.R., 1987. Global uniform asymptotic wave-equation solutions for large wavenumbers, *Ann. Phys.,* **180,** 108–151.

Klauder, J.R., 1988. New asymptotics for old wave equations, *Science,* **239,** 760–762.

Maslov, V.P. & Fedoriuk, M.V., 1981. Semi-classical approximation in quantum mechanics, D. Reidel Publ. Co., Dordrecht.

Nolet, G., Montelli, R., Masters, G., Dahlen, F.A. & Hung, S.-H., 2003. Finite frequency tomographys shows a variety of plumes, *EGS-AGU-EUG Joint Assembly, Nice, April 2003* abstract EAE03-A-03146.

Nowack, R.L., 2003. Calculation of syntheic seismograms with Gausian beams, *Pure appl. geophys.,* **160,** 487–507.

Pratt, R.G., Shin, C. & Hicks, G.J., 1998. Gauss-Newton and full Newton methods in frequency-space seismic waveform inversion, *Geophys. J. Int.,* **133,** 341–362.

Thomson, C.J., 1997. Complex rays and wave packets for decaying signals in inhomogeneous, anisotropic and anelastic media, *Studia geoph. et geod.,* **41,** 345–381.

Thomson, C.J., 2001. Seismic coherent states and ray geometrical spreading, *Geophys. J. Int.,* **144,** 320–342.

Thomson, C.J. & Chapman, C.H., 1985. An introduction to Maslov's asymptotic method, *Geophys. J. R. astr. Soc.,* **83,** 143–168.

Thomson, C.J. & Chapman, C.H., 1986. End-point contributions to synthetic seismograms, *Geophys. J. R. astr. Soc.,* **87,** 285–294.

Weber, M., 1988. Computation of body-wave seismograms in absorbing 2-D media using the Gaussian beam method: comparison with exact methods, *Geophys. J.,* **92,** 9–24.

White, B.S., Norris, A., Bayliss A. & Burridge, R., 1987. Some remarks on the Gaussian beam summation method, *Geophys. J. R. astr. Soc.,* **89,** 579–636.

Whittaker, E.T. & Watson, G.N., 1973. *A course of modern analysis,* Cambridge Univ. Press, Cambridge.

APPENDIX A: ASYMPTOTIC FORM OF THE FOURIER SOLUTION (EQ. 4.1) AROUND THE CRITICAL RAY

The p_1 integral of interest for its branch-point contributions to eq. (4.1) is divided into two at p_c and the opposite limits are extended to $\pm\infty$ on the understanding that this will not change the important behaviour. Let

$$\mathrm{Cr}(a, b, \omega) = I_1 + I_2$$
$$= \int_{-\infty}^{p_c} + \int_{p_c}^{\infty} (p_c - p_1)^{\frac{1}{2}} \exp\left\{ \mathrm{i}\omega \left[a\,(p_1 - p_c) + \frac{1}{2} b\,(p_1 - p_c)^2 \right] \right\} dp_1, \tag{A1}$$

where $b < 0$ and a may be positive or negative. Amplitude factors such as $2\mathrm{i}\omega q_1$ and r_2 are taken to be effectively constant near p_c and are therefore moved outside the dp_1 integration in eqs (4.1) and (4.5). Similarly, the phase term $\exp\{\mathrm{i}\omega[\tau^{\mathrm{refl}}(p_c) + p_c(x_1 - x_{1S}) + p_2(x_2 - x_{2S})]\}$ is omitted here.

The required integral definition of the Weber function of order $-\frac{3}{2}$ is

$$D_{-\frac{3}{2}}(z) = \frac{\Gamma\left(-\frac{1}{2}\right)}{2\pi\mathrm{i}} e^{-\frac{1}{4}z^2} \int_{\alpha} s^{\frac{1}{2}} e^{zs - \frac{1}{2}s^2} ds, \tag{A2}$$

where α is a two-sided contour along the negative real s-axis that loops around the branch point (see Abramowitz & Stegun 1965, eq. 19.5.1 and fig. 19.1; Whittaker & Watson 1973, section 16.6). On the lower and upper half of the contour, $\arg(s) = -\pi$ and $\arg(s) = \pi$, respectively, the two parts contribute equally to the total.

Consider integral I_1, in which the positive real root is chosen for $(p_c - p_1)^{\frac{1}{2}}$. Set $t = p_1 - p_c$ and choose $(p_c - p_1)^{\frac{1}{2}} = \mathrm{i}t^{\frac{1}{2}}$. With this choice, selecting $t^{\frac{1}{2}} = -\mathrm{i}|t^{\frac{1}{2}}|$ for $t = (-\infty, 0)$ maintains the value of the integrand and means that the t contour lies just below the negative real t-axis with the same sense as the lower partial path in the Weber function definition. Now deform the contour clockwise to Γ_1 in Fig. A1.

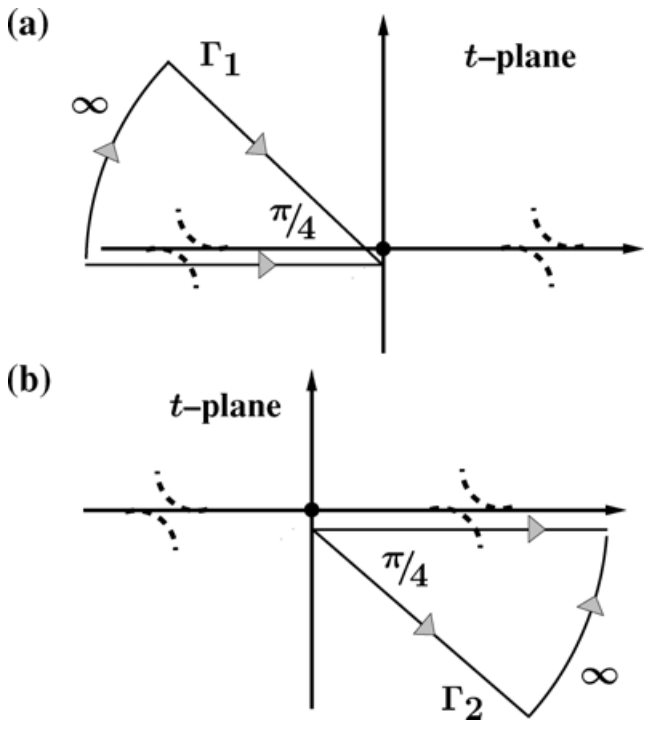

Figure A1. Original and deformed integration paths for recasting the integrals in eq. (A1) into Weber functions defined as in integral eq. (A2). (a) Path Γ_1 appropriate to contribution I_1. (b) Path Γ_2 appropriate to contribution I_2. Also shown with broken lines are possible saddle-points.

The arc at ∞ contributes nothing for all a and along the radial line we have $t = |t|e^{-\mathrm{i}5\pi/4} = se^{-\mathrm{i}\pi/4}$. The lower branch $-\mathrm{i}|s^{\frac{1}{2}}|$ is again taken for $s^{\frac{1}{2}}$, keeping the integrand unchanged and the s contour just below the negative real s -axis. The integral becomes

$$I_1 = e^{\mathrm{i}\pi/8}\int_{-\infty}^{0} s^{\frac{1}{2}}\exp\left(\omega a e^{\mathrm{i}\pi/4}s - \frac{1}{2}\omega|b|s^2\right)ds, \tag{A3}$$

where the sign of b has been considered. A simple positive scaling $t = (\omega|b|)^{\frac{1}{2}}s$ now brings this integral into that of the lower partial path for the Weber function and accounting for a factor of 2 yields

$$I_1 = \frac{\pi\mathrm{i}}{\Gamma(-\frac{1}{2})}\frac{1}{(\omega|b|)^{\frac{3}{4}}}e^{\mathrm{i}\pi/8}e^{\mathrm{i}\omega a^2/4|b|}D_{-\frac{3}{2}}\left[(\omega/|b|)^{\frac{1}{2}}\,e^{\mathrm{i}\pi/4}a\right]. \tag{A4}$$

Now consider integral I_2 and note first the necessity that $(p_c - p_1)^{\frac{1}{2}} = \mathrm{i}|(p_c - p_1)^{\frac{1}{2}}|$ on account of the radiation condition in the lower medium as $z \to \infty$. Set $t = p_1 - p_c$ and choose $(p_c - p_1)^{\frac{1}{2}} = \mathrm{i}t^{\frac{1}{2}}$, meaning that the positive real root of $t^{\frac{1}{2}}$ is used. Now deform the contour to Γ_2 in Fig. A1. The arc at ∞ contributes nothing for all a and along the radial line we have $t = |t|e^{-\mathrm{i}\pi/4} = se^{-\mathrm{i}\pi/4}$. The unchanged integral becomes

$$I_2 = e^{\mathrm{i}\pi/8}\int_{0}^{\infty} s^{\frac{1}{2}}\exp\left(\omega a e^{\mathrm{i}\pi/4}s - \frac{1}{2}\omega|b|s^2\right)ds, \tag{A5}$$

where again the positive root $s^{\frac{1}{2}}$ is used and the sign of b has been considered. Now setting $s = -t$ and $s^{\frac{1}{2}} = -\mathrm{i}t^{\frac{1}{2}}$, with $t^{\frac{1}{2}}$ interpreted as the upper root $\mathrm{i}|t^{\frac{1}{2}}|$, preserves the integrand and leads to the upper half of the contour integral defining the Weber function. After the simple scaling by $(\omega|b|)^{\frac{1}{2}}$ one finds

$$I_2 = \frac{\pi\mathrm{i}}{\Gamma\left(-\frac{1}{2}\right)}\frac{1}{(\omega|b|)^{\frac{3}{4}}}e^{\mathrm{i}\pi/8}e^{\mathrm{i}\frac{1}{4}\omega a^2/|b|}D_{-\frac{3}{2}}\left[(-\omega/|b|)^{\frac{1}{2}}e^{\mathrm{i}\pi/4}a\right]. \tag{A6}$$

The net result is that the integral (eq. A1) can be written

$$\begin{aligned}\mathrm{Cr}(a,b,\omega) &= \frac{\pi\mathrm{i}}{\Gamma\left(-\frac{1}{2}\right)}\frac{1}{(\omega|b|)^{\frac{3}{4}}}e^{\mathrm{i}\pi/8}e^{\mathrm{i}\frac{1}{4}\omega a^2/|b|}\left\{D_{-\frac{3}{2}}[(\omega/|b|)^{\frac{1}{2}}e^{\mathrm{i}\frac{\pi}{4}}a] + \mathrm{i}D_{-\frac{3}{2}}[-(\omega/|b|)^{\frac{1}{2}}e^{\mathrm{i}\frac{\pi}{4}}a]\right\}\\ &= \frac{2\sqrt{2}\pi\mathrm{i}}{\Gamma\left(-\frac{1}{2}\right)}\frac{1}{(\omega|b|)^{\frac{3}{4}}}e^{\mathrm{i}3\pi/8}e^{\mathrm{i}\frac{1}{4}\omega a^2/|b|}D_{\frac{1}{2}}[-(\omega/|b|)^{\frac{1}{2}}e^{-\mathrm{i}\frac{\pi}{4}}a],\end{aligned} \tag{A7}$$

where the final form (eq. A7) is obtained using an identity for Weber functions (Whittaker & Watson 1973 section 16.511, p. 348) that was also used by Brekhovskikh (1980, p. 271). Unfortunately, the Weber function argument in eq. (A7) appears to place it in material disagreement with the related eq. (31.18) of Brekhovskikh (1980, p. 271). Although complete correspondence is not expected, the complex argument of the Weber function $D_{\frac{1}{2}}$ should be compatible (η of Brekhovskikh 1980, measures offset from the critical distance with the same sign as a here). Brekhovskikh (1980) divides the total solution into two parts, ψ_{refl} and ψ_{lat} (eqs 31.17 and 31.10, respectively, of Brekhovskikh 1980). In the pre-critical region the former is used alone and is recast as (Brekhovskikh 1980 eq. 31.18). In the post-critical region the two are added and according to the comment after (Brekhovskikh 1980, eq. 31.18) the net result is the same (i.e. eq. 31.18 applies throughout). However, it is not difficult to verify that choosing the minus sign in (Brekhovskikh 1980, eq. 31.17) and adding (Brekhovskikh 1980, eq. 31.10) does not in fact yield (Brekhovskikh 1980, eq. 31.18) as stated. The addition process is not in question and it is notable that if the $\pm$ signs in (Brekhovskikh 1980, eq. 31.17) are reversed then a common result is indeed obtained in both the pre- and post-critical regions, and furthermore its Weber function argument agrees with eq. (A7) above. Equivalently, the relative signs of $D_{-\frac{3}{2}}$ terms in the previous line would then agree with Brekhovskikh (1980, eq. 31.17).

The derivation given in this appendix is sufficiently brief that any error will hopefully be revealed soon, but either way the important conclusion is that the branch-point effect in a boundary-layer around the critical ray is described by a canonical wavefunction denoted here by $\mathrm{Cr}(a, b, \omega)$ and which can be cast in terms of Weber functions.

APPENDIX B: COHERENT-STATE BRANCH-POINT CONTRIBUTIONS VIA EQS (4.9) AND (4.11)

For the case $p_1' > p_c$ displayed in Fig. 4(a) the p_1 integral of interest for its branch-point contribution to eq. (4.9) is

$$I = \int_{-\infty}^{p_c}(p_c - p_1)^{\frac{1}{2}}\exp[\mathrm{i}\omega a(p_1 - p_c)]\,dp_1, \tag{B1}$$

where $\Re(a) > 0$ and $\Im(a) < 0$ as defined just following eq. (4.10). Integral eq. (B1) is the contribution from the lower portion of the branch cut and there is an equal contribution from the upper portion. The objective is to exploit the standard integral used by Thomson & Chapman (1986, p. 291)

$$\int_0^\infty x^2\exp(\mathrm{i}\beta x^2)\,dx = \frac{\exp\left[\mathrm{i}\frac{3\pi}{4}\mathrm{sgn}(\beta)\right]\pi^{\frac{1}{2}}}{4|\beta|^{\frac{3}{2}}}, \tag{B2}$$

where β is real. To this end the new variable $\eta = (p_c - p_1)^{\frac{1}{2}}$ is introduced and the path of integration in eq. (B1) is then deformed to the radial line $\eta = |\eta| \exp[-\mathrm{i}\frac{1}{2}\arg(a)] = \bar{\eta}\exp[-\mathrm{i}\frac{1}{2}\arg(a)]$ plus a negligible arc at infinity. The result from the new radial line is that

$$I = 2\exp\left[-\mathrm{i}\frac{3}{2}\arg(a)\right]\int_0^\infty \bar{\eta}^2 \exp(-\mathrm{i}\omega|a|\bar{\eta}^2)\, d\bar{\eta} = \frac{\pi^{\frac{1}{2}}}{2}\frac{\exp\left(-\mathrm{i}\frac{3\pi}{4}\right)}{(\omega a)^{\frac{3}{2}}}, \tag{B3}$$

where, as throughout, it is assumed ω is positive real.

For the case $p_1' < p_c$ displayed in Fig. 4(b) the p_1 integral of interest for its branch-point contribution to eq. (4.9) is

$$I = \int_{p_c}^\infty (p_c - p_1)^{\frac{1}{2}} \exp[\mathrm{i}\omega a(p_1 - p_c)]\, dp_1, \tag{B4}$$

where now $\Re\,(a) > 0$ and $\Im\,(a) > 0$. Also $(p_c - p_1)^{\frac{1}{2}} = \mathrm{i}|(p_c - p_1)^{\frac{1}{2}}|$ and integral eq. (B4) is again a semi-contribution coming from the lower portion of the branch cut. Now the new variable $\eta = |(p_c - p_1)^{\frac{1}{2}}| = -\mathrm{i}(p_c - p_1)^{\frac{1}{2}}$ is introduced and the path of integration in eq. (B4) is then deformed to the radial line $\eta = |\eta| \exp[-\mathrm{i}\frac{1}{2}\arg(a)] = \bar{\eta}\exp[-\mathrm{i}\frac{1}{2}\arg(a)]$ plus a negligible arc at infinity. Note $\arg(a)$ is positive in this case. The result from the new radial line is that

$$I = 2\mathrm{i}\exp\left[-\mathrm{i}\frac{3}{2}\arg(a)\right]\int_0^\infty \bar{\eta}^2 \exp(\mathrm{i}\omega|a|\bar{\eta}^2) d\bar{\eta} = \mathrm{i}\frac{\pi^{\frac{1}{2}}}{2}\frac{\exp\left(\mathrm{i}\frac{3\pi}{4}\right)}{(\omega a)^{\frac{3}{2}}}. \tag{B5}$$

Because $\mathrm{i}\exp(\mathrm{i}\frac{3\pi}{4}) = \exp(-\mathrm{i}\frac{3\pi}{4})$ the contributions of eqs (B5) and (B3) have the same functional form, which is important to note for subsequent p_1' integration in the inverse CST (eq. 2.7).

The remaining case $p_1' \approx p_c$ can be addressed either starting from the uniformly-asymptotic form (eq. 4.11) or more directly using integral (eq. 4.9). Note that expansion (eq. 4.10) does not preclude the possibility $p_1' \approx p_c$ and that, provided $\Re(a) > 0$ and the saddle point is far removed from p_c, the isolated branch-point contributions to eqs (4.9) and (4.11) will have the same form as eqs (B3) and (B5). In fact, when $p_1' = p_c$ the exponential-growth difficulty referred to after eq. (4.10) does not arise and the straightforward real-axis approach applies. Also, because eq. (4.11) was derived only near the critically-reflected real ray, an extra step in the argument is needed to explain how its branch-point contributions may be used further into the post-critical region and for this reason it may be preferable to start from eq. (4.9).

In order to facilitate the CS synthesis discussion in Section 4.6, it is desirable to collect together the p_1' -dependent branch-point terms contributing to the inverse CST (eq. 2.7). On using the explicit form of a given after eq. (4.10) one finds that the final isolated head wave signal depends upon the p_1' integral

$$\int_{-\infty}^\infty \frac{\exp\left[-(\omega/2\Omega)(p_c - p_1')^2\right]}{\left[x_1 - x_{1S} - X_c + \mathrm{i}\Omega^{-1}(p_c - p_1')\right]^{\frac{3}{2}}}\, dp_1'. \tag{B6}$$

This does not integrate exactly to give a simple form independent of Ω. Thus, just as with the saddle-point contributions discussed in Section 4.6, the CS method gives a new asymptotic representation of the head wave in which Ω dependence exists but is expected to be weak. In fact, the main contribution to eq. (B6) comes from near p_c and in this neighbourhood the denominator can be approximated by its real part. Then the Gaussian p_1' integral is easily performed and the result agrees with the standard Fourier approach in Thomson & Chapman (1986). An asymptotic expansion in a particular functional form is unique (Jeffreys & Jeffreys 1980, p. 500) and eq. (B6) is simply an equally valid alternative to the (simpler) standard Fourier result. Their differences will continue into the higher terms in inverse powers of frequency, presumably compensating for any differences in the leading term and, with the usual limitations of such expansions, providing a closer representation of the true head wave.